Archival Report

Biological Psychiatry: GOS

Electroencephalographic Microstates During Sleep and Wake in Schizophrenia

Michael Murphy, Chenguang Jiang, Lei A. Wang, Nataliia Kozhemiako, Yining Wang, the GRINS Consortium, Jun Wang, Jen Q. Pan, and Shaun M. Purcell

ABSTRACT

BACKGROUND: Aberrant functional connectivity is a hallmark of schizophrenia. The precise nature and mechanism of dysconnectivity in schizophrenia remains unclear, but evidence suggests that dysconnectivity is different in wake versus sleep. Microstate analysis uses electroencephalography (EEG) to investigate large-scale patterns of coordinated brain activity by clustering EEG data into a small set of recurring spatial patterns, or microstates. We hypothesized that this technique would allow us to probe connectivity between brain networks at a fine temporal resolution and uncover previously unknown sleep-specific dysconnectivity.

METHODS: We studied microstates during sleep in patients with schizophrenia by analyzing high-density EEG sleep data from 114 patients with schizophrenia and 79 control participants. We used a polarity-insensitive *k*-means analysis to extract a set of 6 microstate topographies.

RESULTS: These 6 states included 4 widely reported canonical microstates. In patients and control participants, falling asleep was characterized by a shift from microstates A, B, and C to microstates D, E, and F. Microstate F was decreased in patients during wake, and microstate E was decreased in patients during sleep. The complexity of microstate transitions was greater in patients than control participants during wake, but this reversed during sleep.

CONCLUSIONS: Our findings reveal behavioral state–dependent patterns of cortical dysconnectivity in schizophrenia. Furthermore, these findings are largely unrelated to previous sleep-related EEG markers of schizophrenia such as decreased sleep spindles. Therefore, these findings are driven by previously undescribed sleep-related pathology in schizophrenia.

https://doi.org/10.1016/j.bpsgos.2024.100371

Evidence from multiple studies supports the idea that schizophrenia and other psychotic disorders are dysconnection syndromes (1). However, the relationship between dysconnectivity and psychotic disorders remains incompletely understood. Electroencephalography (EEG) is a useful tool for studying brain connectivity because it allows for measurement of cortical activity at millisecond resolution. EEG has been widely used to study the pathophysiology of schizophrenia. These studies have demonstrated that some large-scale neural oscillations are disrupted in schizophrenia. For example, sleep spindles, which are bursts of 11- to 15-Hz activity that occur during N2 sleep, are diminished in patients with schizophrenia (2,3). This sleep spindle deficit may be related to impaired sleep-dependent memory consolidation in patients (4). In addition, alpha waves are slowed and attenuated in patients with schizophrenia compared with control participants, and this may be linked to cognitive deficits (5–7).

In addition to oscillation-based analyses, EEG data can be analyzed topographically. EEG data can be modeled as consisting of a small number of characteristic topographies that persist for tens of milliseconds and then transition to a different characteristic topography (8). These periods of semistable topography are called microstates. Investigators have consistently reported 4 canonical microstates in human EEG data, although studies using high-density EEG have described additional microstates (9,10). While the precise neural correlates of each microstate remain uncertain, it is likely that they overlap with but are distinct from brain networks identified with functional magnetic resonance imaging (11). Microstate topographies, parameters, and transition properties are driven by the coordinated action of meso-scale neural assemblies (9). Therefore, case-control differences in microstates reflect case-related dysconnectivity between populations of cortical neurons.

A growing body of literature describes microstate abnormalities during quiet rest in patients with schizophrenia (12). While the topography of the canonical microstates is essentially unchanged in patients with schizophrenia, microstate duration, occurrence, and transition probabilities are different. During quiet rest, canonical microstate C coverage and occurrence are increased in patients with schizophrenia compared with healthy control participants, while microstates B and D are decreased (12,13). Furthermore, in patients with schizophrenia, there is a higher likelihood of transitioning from microstate D to C and a lower likelihood of the reverse transition than in healthy control participants (13). Finally,

ISSN: 2667-1743

transitions between microstates are relatively unstructured and chaotic in patients with psychotic disorders compared with healthy control participants (14). Overall, the literature in this area is somewhat unclear however, and its interpretation is complicated by a lack of consensus around analysis parameters and the fact that there have been few large-scale studies.

Previous studies of EEG microstates in patients with schizophrenia have used data from quiet rest (12). However, one of the largest and most well-replicated EEG abnormalities in schizophrenia is decreased sleep spindles. Microstate topography is not significantly different in sleep and wake in healthy control participants (15,16). Average duration for all microstates is increased during sleep (15). Brodbeck *et al.* reported that N2 sleep was associated with an increase in microstate B (15), and Brechet *et al.* reported that microstates C and D were increased in non–rapid eye movement (NREM) sleep and that microstate C was linked to dreaming (16).

We conducted a large, high-density EEG study of sleep in patients with schizophrenia and found that patients had decreased sleep spindles compared with control participants (3). Here, we used an overlapping dataset to conduct a large study of EEG microstates in patients with schizophrenia as well as the first study of sleep-related microstates in this population. We hypothesized that there would be state-dependent case-control differences in microstate parameters and that microstates C and E, which resemble the topography of sleep spindles, would be decreased in patients compared with control participants. We also hypothesized that transitions between microstates would be more chaotic in patients.

METHODS AND MATERIALS

Participants and Procedure

The data were collected as part of the GRINS (Global Research Initiative of Neurophysiology on Schizophrenia) study, a collaboration between the Broad Institute of Harvard and Massachusetts Institute of Technology and Wuxi Mental Health Center. All participants provided written informed consent. The study was approved by the Harvard T.H. Chan School of Public Health Office of Human Research Administration (IRB18-0058) and the institutional review board of Wuxi Mental Health Center (WXMHCIRB2018LLKY003). All study procedures complied with the Declaration of Helsinki. For full details of data collection, see Kozhemiako *et al.* (3). We analyzed data from 114 patients with schizophrenia and 79 age-matched control participants. Demographic information is provided in Table 1. An unpaired *t* test showed that there was no statistically significant group difference in age between groups (p = .14), and a χ^2 test showed that there was no statistically significant difference in sex (p = .61). All patients were taking antipsychotic medication; of 114 patients, 29 were taking mood stabilizers, 29 were taking benzodiazepines and/or antihistamines, and 4 were taking selective serotonin reuptake inhibitors. Given the low number of patients taking nonantipsychotic medications, we limited our medication-related analyses to antipsychotics. All participants were between the ages of 18 and 45 years. Patients were recruited from inpatient services at Wuxi Mental Health Center, and control participants were recruited through advertisements posted in the community. Exclusion criteria were electroconvulsive therapy in the past 6 months; current barbiturate use; a history of sleep disorders; a hearing threshold above 45 dB at 1000 Hz as determined by an audiometer; serious neurological, medical, or psychiatric illness (control participants only); and pregnancy. Exclusion criteria were assessed by study staff at the time of enrollment (questionnaires and audiometric testing). The study protocol consisted of multiple visits including cognitive testing and symptom assessment using the Positive and Negative Syndrome Scale (17).

Table 1. Demographic and Clinical Characteristics of the Study Population

Characteristic	Control Group	SZ Group
Sample Size	79	114
Age, Years	32.9 (0.7)	34.4 (0.7)
Sex, Female/Male	29/50	46/68
Chlorpromazine Equivalents, mg	0	673.3 (26.0)
PANSS		
Positive factor	–	2.3 (0.1)
Negative factor	–	2.5 (0.1)
Excited factor	–	1.8 (0.1)
Disorganized factor	–	2.3 (0.1)
Depressed factor	–	1.6 (0.1)

Values are presented as mean (SEM) or *n*. PANSS factors were derived from Wallwork *et al.* (41).

PANSS, Positive and Negative Syndrome Scale; SZ, schizophrenia.

Electroencephalography

EEG data were collected at 500 Hz using a custom-designed cap (64 Ag-AgCl channels; Brain Products GmbH) with a left clavicle ground electrode, a central forehead reference electrode, and vertical and horizontal electrooculogram channels. Impedances were <10 kW. We recorded 7 minutes of eyes-closed EEG, and then participants were allowed to sleep naturally. Recordings were monitored by onsite staff. Following acquisition, bad channels were identified with a semi-automated procedure and spline interpolated (3). Independent component analysis was used to remove ocular and electrocardiogram artifacts. Data was re-referenced to the average reference, filtered between 0.3 and 35 Hz, and downsampled to 200 Hz. Sleep staging, spindle detection, slow oscillation detection, and spindle-slow oscillation coupling were performed as in Kozhemiako *et al.* (3). For case-control sleep parameter comparisons, see Table S1. For band-specific analysis, we used the following frequency bands: slow (0.5–1 Hz) and sigma (11–15 Hz). Spindle detection for slow spindles was done using a wavelet centered on 11 Hz, and fast spindles were detected using a similar wavelet centered on 15 Hz (18).

Microstate Analysis

Microstate analyses were performed using Luna (http://zzz.bwh.harvard.edu/luna/), an open-source software package developed by SMP. Because using separate microstate topographies in group comparisons of microstate parameters can lead to increased rates of type I error, we used a single set of topographies to model all the data (19). From each

participant and behavioral state (quiet rest, N2, N3, and REM sleep), we extracted data from 500 points corresponding to local maxima in the global field power. For sleep states, we used an automated, diagnosis-blind procedure to randomly select 15 minutes of contiguous sleep for each stage for broad comparability with the duration of the quiet rest recordings. Resting-state microstate topographies can be reliably extracted from such reduced datasets (15). Preliminary analyses using the CARTOOL metacriterion (Denis Brunet, cartool-community.unige.ch) indicated that $k = 6$ would be appropriate (20). We used a polarity-insensitive *k*-means analysis to extract 6 microstate topographies from broadband quiet rest data and sigma and slow-filtered N2 data. We combined all maps into a library and merged maps that were highly correlated ($r > 0.75$). This procedure yielded a set of 6 maps, which we fitted back into the EEG data. Each time point was assigned a microstate label, and segments were rejected if they were >20 ms. We used the same set of 6 microstates for all analyses. We calculated 4 microstate parameters. Coverage was the portion of the record that was covered by a microstate. Duration was the average duration of a microstate when it occurred. Explained variance was how much of the variance in the EEG data was accounted for by each microstate. Occurrence was how often a microstate occurred per second. To examine microstate sequence transition and complexity properties, we removed information about duration from the sequence of microstates. We calculated Lempel-Ziv-Welch complexity for these sequences (21). We compared the observed probability of transitioning from one microstate to another against what would be expected given a random distribution of microstate labels (with the constraint of no identical contiguous states). We examined how likely each microstate sequence of length 4 would be to occur given a random distribution of labels (14). We analyzed sequences of length 4 because previous work suggested that there would be case/control differences at this length while still having only a few hundred possible sequences (14).

Statistics

We used unpaired *t* tests, Bonferroni corrected for multiple comparisons, to compare microstates. To test for associations between NREM EEG waveforms and microstate metrics, we fit a series of pairwise linear models comparing all NREM EEG waveform metrics (dependent variables) against microstate metrics (predictor variables), either separately in cases or controls or in the combined sample but with disease state as a binary covariate. We used the Freedman-Lane permutation procedure to correct for multiple testing, controlling the experiment-wide false positive rate but allowing for the correlational structure between all NREM metrics and all microstate metrics as well as the presence of a nuisance variable (i.e., disease state in the combined analysis) (22,23). We performed $24 \times 240 = 5760$ tests (from 24 = 6 states × 5 microstate metrics and 240 = 12 channels × 2 spindle frequencies × 8 spindle metrics + 12 channels × 4 slow oscillation metrics). We created 10,000 null datasets following the Freedman-Lane approach to derive both a pointwise empirical significance per metric and a corrected empirical significance, adjusting for all tests, based on the empirical distribution of the maximum *t* statistics under the null. We report as significant only tests with an adjusted *p* level (p_{adj}) < .05.

RESULTS

Microstate F Duration Is Decreased in Patients With Schizophrenia During Quiet Rest

Previous reports described increased microstate C and decreased microstate D during resting state in patients with schizophrenia compared with healthy control participants (13). Most of these reports used different sets of microstates for patients and control participants. However, using separate sets of microstates greatly inflates type I error rates (19). We attempted to replicate these previous findings using a more methodologically rigorous approach. Our microstate segmentation produced a set of 6 microstates, which included the canonical 4 microstates (Figure 1). We compared the coverage, duration, explained variance, and occurrence of the 6 microstates in cases and controls during quiet wake (Figure 2). Unlike previous results, we did not find any statistically significant differences in any of these parameters for microstates C and D (all $p_{adj} > .05$). We did find decreased microstate F duration in cases (46.5 ms [SEM 0.5])

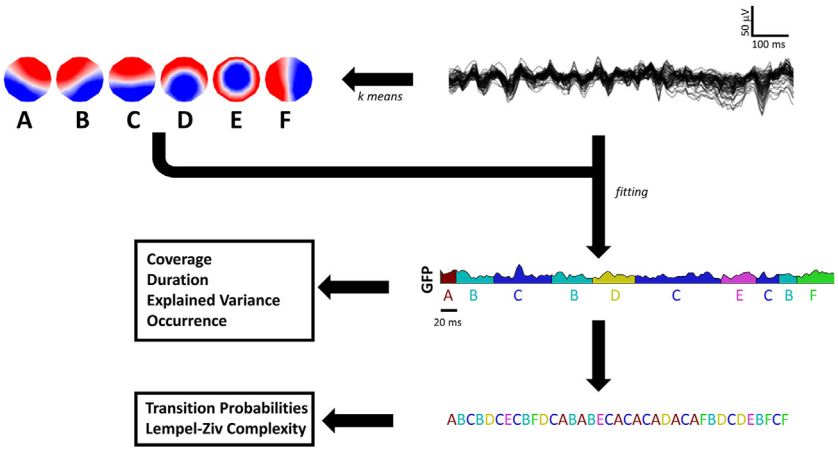

Figure 1. Microstate analysis pipeline. A modified *k*-means analysis was used to produce a set of 6 microstate topographies labeled A to F. These microstates were then backfit into the electroencephalography data. These fittings were then used to calculate microstate coverage, duration, explained variance, and occurrence. Information about duration was removed from the data to yield a sequence of microstates. These sequences were used to calculate transition probabilities and Lempel-Ziv complexity. GFP, global field power.

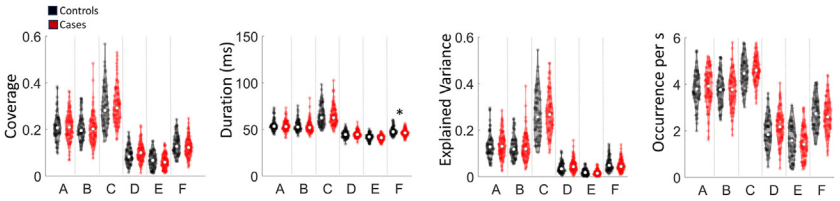

Figure 2. Microstate parameters in cases and controls during quiet waking. Black left violins are control data, and red right violins are patient data. The horizontal axes indicate microstate labels. Microstates are separated with gray dotted lines. For coverage, the vertical axis is the proportion of the data covered by a given microstate. For duration, the vertical axis is the mean duration in milliseconds. For explained variance, the vertical axis is the proportion of the variance in the original data explained by each microstate. For occurrence, the vertical axis is how frequently each microstate occurs per second. $^{*}p_{adjusted} < .05$.

compared with controls (48.2 ms [SEM 0.5]) (p_{adj} = .011, Hedges' g = 0.46). We found no statistically significant correlations between any microstate feature and chlorpromazine equivalents (all ps > .11). There were nominally significant positive correlations between illness duration and microstate A parameters and negative correlations between illness duration and microstate E parameters but not after correction for multiple comparisons (all p_{adj} > .05). There were no statistically significant relationships between symptom scores and microstate features (all p_{adj} > .06).

Microstate E Is Decreased in Patients With Schizophrenia During NREM Sleep

For both cases and controls, there was a clear shift from microstates A, B, and C during quiet wake to microstates D and E during sleep and, to a lesser extent, microstate F during NREM sleep (Figure 3A). Next, we compared data from cases and controls during N2, N3, and REM sleep. We found statistically significant decreases in microstate E duration in cases compared with controls during N2 sleep (50.6 ms [SEM 0.4] vs. 52.3 ms [SEM 0.4], p_{adj} = .014, Hedges' g = 0.45) and N3 sleep (54.2 ms [SEM 0.4] vs. 57.3 ms [SEM 0.6], p_{adj} = .0001, Hedges' g = 0.66) (Figure 3B). We found that a similar decrease in microstate E explained variance in cases compared with controls in both N2 sleep (0.069 [SEM 0.003] vs. 0.085 [SEM 0.003], p_{adj} = .0014, Hedges' g = 0.55) and N3 sleep (0.057 [SEM 0.002] vs. 0.070 [SEM 0.003], p_{adj} = .0041, Hedges' g = 0.51). We also found an increase in microstate C occurrence during N3 sleep in cases compared with controls (3.3 states/s [SEM 0.04] vs. 3.1 states/s [SEM 0.04], p_{adj} = .018, Hedges' g =

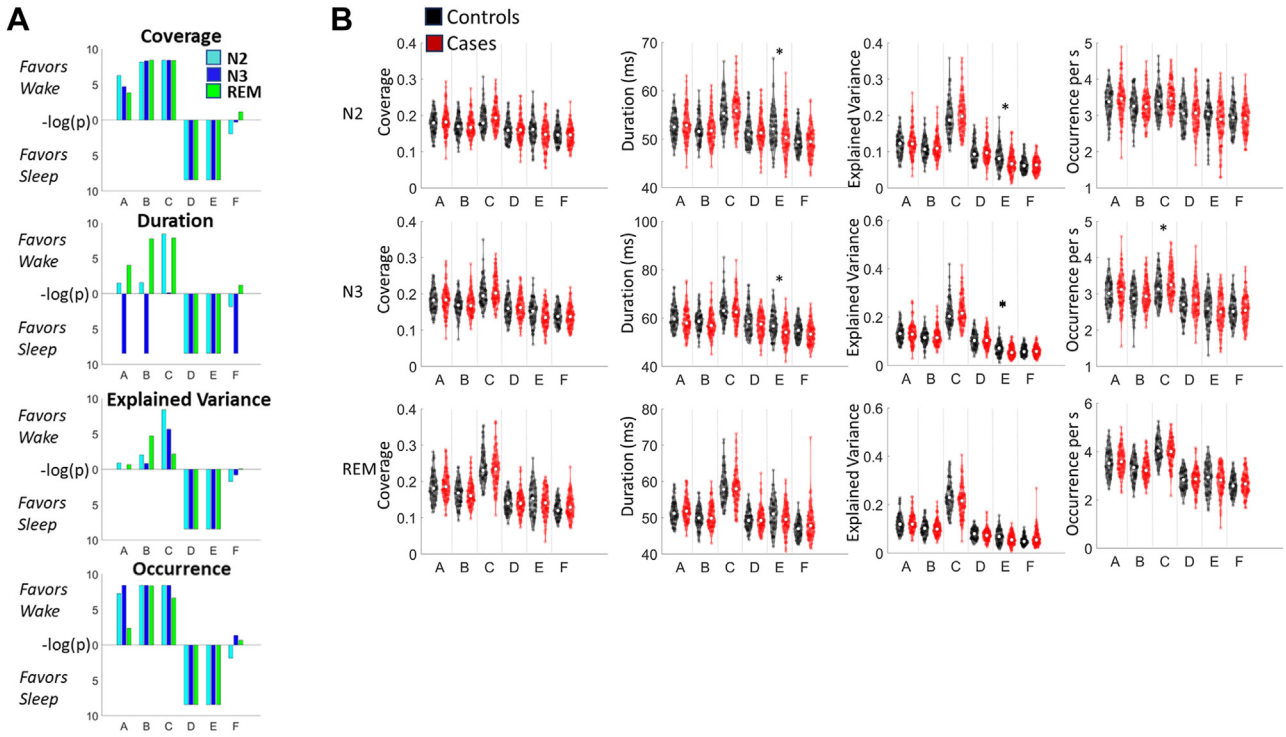

Figure 3. Microstates during sleep in cases and controls. **(A)** There is a shift from microstates A, B, and C during wake to D, E, and F during sleep. For each parameter (coverage, duration, explained variance, and occurrence), there is a bar graph of the −log(p) from paired t tests between data from quiet rest and N2 sleep (light blue), N3 sleep (dark blue), and rapid eye movement (REM) sleep (green) in healthy control participants. For case data, which are highly similar, see the Supplement. **(B)** Microstate parameters in cases (red, right violins) and controls (black, left violins) during sleep. The horizontal axes indicate microstate labels. Microstates are separated with gray dotted lines. For coverage, the vertical axis is the proportion of the data covered by a given microstate. For duration, the vertical axis is the mean duration in milliseconds. For explained variance, the vertical axis is the proportion of the variance in the original data explained by each microstate. For occurrence, the vertical axis is how frequently each microstate occurred per second. $^{*}p_{adjusted} < .05$.

0.44). We found no statistically significant difference between any microstate parameters during REM sleep. Overall, we found that the explained variance of the set of microstates was higher in sleep than in quiet rest (Figure S1).

Sigma Band–Specific Microstate Differences in N2 Sleep in Schizophrenia

We investigated whether sigma band–filtered EEG data (11–15 Hz bandpass) from N2 sleep would show differences between cases and controls (Figure 4A). We found multiple statistically significant differences in microstate parameters. The explained variance for microstate A was increased in cases compared with controls (0.11 [SEM 0.003] vs. 0.09 [SEM 0.003], p_{adj} = .027, Hedges' g = 0.42). Microstate C coverage (0.168 [SEM 0.004] vs. 0.142 [SEM 0.004], $p_{adj} < 10^{-5}$, Hedges' g = 0.75), duration (128.6 ms [SEM 1.6] vs. 118.9 ms [SEM 1.3], p_{adj} = .0001, Hedges' g = 0.64), explained variance (0.13 [SEM 0.004] vs. 0.10 [SEM 0.005], $p_{adj} < .0001$, Hedges' g = 0.68), and occurrence (1.30 states/s [SEM 0.01] vs. 1.18 states/s [SEM 0.01], $p_{adj} < 10^{-6}$, Hedges' g = 0.80) were increased in cases compared with controls. Microstate D duration was decreased in cases compared with controls (145.9 ms [SEM 2.1] vs. 155.3 ms [SEM 2.6], p_{adj} = .028, Hedges' g = 0.42), as was microstate F coverage (0.163 [SEM 0.003] vs. 0.187 [SEM 0.004], $p_{adj} < 10^{-5}$, Hedges' g = 0.74), duration (139.1 ms [SEM 1.2] vs. 152.8 ms [SEM 2.0], $p_{adj} < 10^{-7}$, Hedges' g = 0.92), explained variance (0.07 [SEM 0.002] vs. 0.08 [SEM 0.003], $p_{adj} < .0001$, Hedges' g = 0.65), and occurrence (1.16 states/s [SEM 0.02] vs. 1.22 states/s [SEM 0.01], p_{adj} = .015, Hedges' g = 0.45). N3 sleep is dominated by slow oscillations, although these oscillations have not been as robustly linked to schizophrenia as spindles. Therefore, we examined whether slow band–filtered (0.5–1 Hz) data would show case-control differences. We did not find any statistically significant differences in microstate parameters in these data.

We investigated whether there were relationships between microstate parameters and slow oscillations, slow spindles, and fast spindles (Figure 4B). Controlling for case-control status, we found that microstate D was positively correlated with both slow and fast spindle amplitude, and microstate E was negatively correlated with fast spindle amplitude. Microstates A and F were only related to spindles while the other microstates were related to both spindles and slow oscillations. For each microstate-parameter pair, all statistically significant relationships were in the same direction. Our results show that there is not a single spindle microstate or microstates. There were no statistically significant differences in correlations between cases and controls (all $p_{adj} > .05$). The full set of relationships and group-specific analyses are presented in the Supplement.

Complexity of Microstate Sequences Differs in Cases Versus Controls

Compared with a model of random transitions dictated by the distribution of microstate labels, microstate transition probabilities are highly nonrandom (Figure 5). Microstates A and B were relatively unlikely to transition between each other and instead were more likely to transition to microstates C and F than would be expected by chance. Microstates C and F were less likely to transition to each other.

We calculated the Lempel-Ziv complexity (LZW) for all microstate sequences in broadband EEG data (Figure 5). For each condition and behavioral state, we rejected values that were >3 scaled median absolute deviations from the median. Multivariate analysis of variance showed main effects of behavioral state ($F_{3,722}$ = 646.1, $p < 10^{-100}$) and case/control status ($F_{1,771}$ = 3.81, $p < .05$) and a statistically significant interaction between behavioral state and case/control status ($F_{3,722}$ = 6.99, $p < 10^{-4}$). Post hoc testing showed that during quiet wake, case LZW (0.283 [SD 0.02]) was greater than control LZW (0.276 [SD 0.02]) (p_{adj} = .04). However, during N2 and N3 sleep, control LZW (0.2463 [SD 0.0009] and 0.2480 [SD 0.0012]) was greater than case LZW (0.2457 [SD 0.0015] and 0.2470 [SD 0.0018]). The Hedges' g values for these case-control differences were 0.35 for quiet rest, 0.47 for N2 sleep, and 0.63 for N3 sleep.

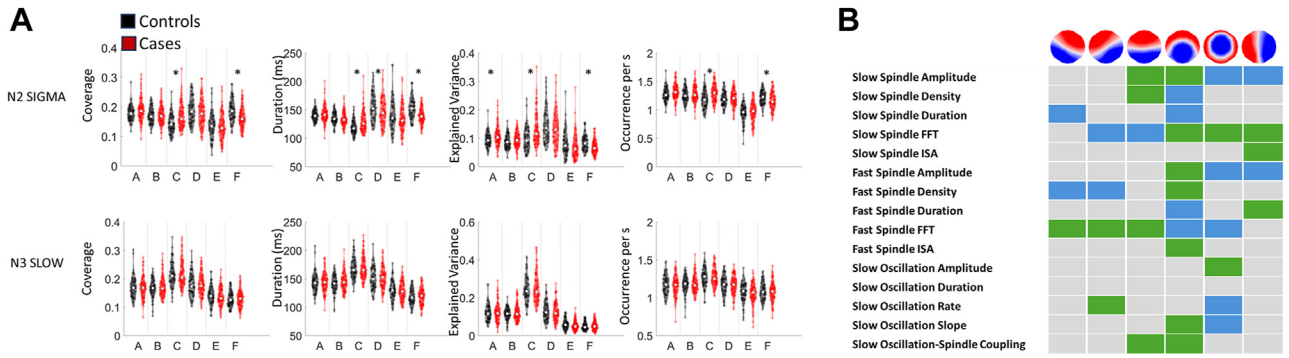

Figure 4. Microstate parameters during sigma-filtered N2 sleep show case-control differences and are related to non–rapid eye movement electroencephalography (EEG) waveforms. **(A)** Microstate parameters in cases (red, right violins) and controls (black, left violins) from sigma-filtered N2 data and slow-filtered N3 data from both cases and controls. *$p_{adjusted} < .05$. **(B)** Microstates during N2 sleep are associated with non–rapid eye movement EEG waveforms. Each row corresponds to a different non–rapid eye movement EEG metric. Each column corresponds to the given microstate in sigma-filtered data. Gray squares indicate no statistically significant association ($p_{adjusted} > .05$). Green indicates a statistically significant positive interaction between at least one microstate parameter (coverage, duration, explained variance, and/or occurrence) and that EEG element of sleep. Blue indicates a statistically significant negative interaction. FFT, fast Fourier transform; ISA, integrated spindle activity.

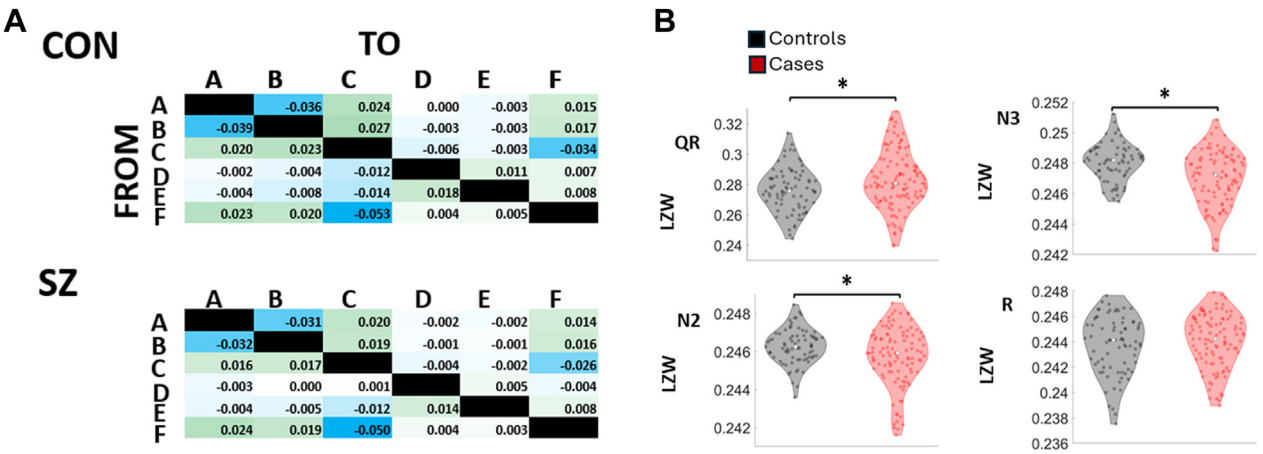

Figure 5. Microstate transitions are nonrandom and differ in cases and controls. **(A)** The top row of matrices shows the difference in transition probabilities observed minus what would be expected under random transitions in controls for broadband data. Blue is less than random, and green is more than random. The second row shows the same analysis for cases. **(B)** The Lempel-Ziv complexity (LZW) of microstate sequences is greater in cases than controls during wake and lower than controls during non–rapid eye movement sleep. Violin plots for mean LZW across all microstates for each behavioral state for cases (red, right) and controls (black, left). *$p < .05$. CON, control; QR, quiet rest; SZ, schizophrenia.

DISCUSSION

To our knowledge, we conducted the largest study to date of EEG microstates in sleep and the first study of sleep-related microstate abnormalities in patients with schizophrenia. Six microstates, which included 4 widely reported canonical microstates, were the optimal way to model the data. Consistent with previous reports, microstates derived from wake data were able to adequately model sleep data. Microstate parameters were modulated by behavioral state and case-control status in a frequency-dependent manner. Contrary to our hypothesis, microstate C was statistically significantly increased during NREM sleep in patients compared with control participants. We did not find evidence for symptom, illness duration, or medication effects on microstate parameters in patients with schizophrenia. Microstates D and E were associated with NREM EEG waveforms. Microstate transitions were nonrandom, and transition structure was more complicated in cases than in controls during wake, but this reversed during sleep.

Microstate Topography Reflects Nonspecific Cortical Connectional Architecture

Our findings are consistent with previous work that has reported the presence of canonical microstate topographies in EEG data collected during sleep and from patients with schizophrenia (9). Most of the EEG signal is produced by the summed action of excitatory and inhibitory postsynaptic potentials on layer V pyramidal cell bodies (24). The sheet-like geometry of this layer allows for the coordinated action of these neurons to sum to produce a measurable signal. During wake, microstate topography is largely driven by alpha activity (25). Alpha waves are initiated and shaped by the interaction of multiple cortical and thalamic pacemakers (26,27). However, during sleep, alpha is diminished compared with spindle and delta activity. Sleep spindles are triggered by input from the thalamic reticular nucleus to the cortex while delta activity is primarily under cortical control and only somewhat influenced by the thalamus (28,29). These different behavioral states with distinct oscillatory signatures driven by disparate cortical and subcortical pacemakers nonetheless produce similar microstate topographies (15). The hypothesis of a common set of brain activation patterns occurring during sleep and wake is supported by our finding that explained variance was comparable for sleep and wake when using a set of microstates that includes canonical wake-derived topographies. This suggests that microstate topographies reveal a cortical connectional architecture that is used by multiple different types of neural activity across different neuromodulatory milieus (30). This connectional architecture is not disconnected during sleep or grossly altered by schizophrenia. However, relationships between microstate topography and cortical connectivity have not been firmly established (10).

Microstate Parameters Reflect State-Dependent Neural Activity and Schizophrenia Neuropathology

We did not replicate previously reported differences in microstates C and D between cases and controls, perhaps due to methodological differences across studies (13). However, we did find evidence that microstate parameters are modulated by both behavioral state and schizophrenia. Falling asleep is accompanied by a shift from microstates A, B, and C to microstates D, E, and F. Microstate A is associated with coordinated activity in the temporal and insular cortices, microstate B is associated with activity in the occipital cortex, and microstate C is associated with activity in the posterior cingulate and precuneus (11,31). The microstates that are increased in NREM sleep are correlated with activity in the thalamus, posterior cingulate, anterior cingulate, and inferior parietal lobule (11). Our data are consistent with deactivation of visual and auditory networks during N2 and N3 sleep that is partially attenuated during REM. This is consistent with

findings that dream reports from REM sleep are more likely to contain detailed sensory information and that dreaming is associated with activity in these networks and in the precuneus (32). Our finding of increased microstate C in REM compared with NREM sleep is consistent with previous reports that microstate C is associated with dreaming (16). Brodbeck *et al.* (15) found increased microstates A and B and decreased microstate C in N2 sleep compared with wake, N1, and N3 sleep. However, these authors used 4 microstates rather than 6 and excluded data from sleep spindles and slow oscillations.

Case-control microstate parameter differences for microstates F and C were different in sigma-filtered compared with broadband data during N2 sleep. This suggests that the neural activity that gives rise to these microstates performs different functions at different frequency bands. For example, activity in the precuneus (corresponding in part to microstate C) below 5 Hz is important for maintaining NREM sleep, while faster activity in this same region is associated with wakefulness.

When comparing cases with controls, we hypothesized that there would be decreases in microstates C and E given the previously reported decrease in sleep spindles in this population (3). The fact that we found a relative increase in microstate C instead demonstrates that microstate analysis provides a distinct view of brain activity compared with frequency-based EEG analyses. Microstate C was negatively correlated with fast spindle density, which is consistent with decreased spindle amplitude in patients with schizophrenia. There are multiple, complicated relationships between microstates and NREM EEG waveforms. Microstate E was decreased in cases compared with controls in NREM sleep. It was associated with having faster slow spindles and slower fast spindles. We note that the topography for microstate E is intermediate between the slow and fast spindle topographies.

Microstate F is decreased in cases compared with controls in sigma-filtered EEG data from N2 sleep. This microstate is positively correlated with slow spindle–integrated spindle activity and fast spindle duration but negatively correlated with slow and fast spindle amplitude. Our findings suggest that distinct deficits in spindle parameters have distinct neural substrates (18).

Microstate D may be particularly important for sleep because it is correlated with multiple features of spindles. We found case-control microstate duration differences for microstate D in N2 sleep. Therefore, microstate D may reflect the coordinated activity of a large neural assembly that is important for sleep and is impaired in schizophrenia. Source modeling analyses indicate that this assembly includes the anterior cingulate gyrus and insular cortices (11). These regions have previously been identified as origin sites for cortical sleep slow oscillations and sleep spindles (33,34).

Microstate Sequences Are Not Random and Instead Reflect Case-Control Status

Transitions between microstates are complex and nonrandom. The literature is mixed as to whether schizophrenia is associated with increased or decreased complexity of quiet rest EEG data (14,35,36). Different measures of complexity capture different facets of brain function. Complexity analyses performed on microstate sequences describe the relationships between large brain networks. Our findings indicate behavioral state–dependent case-control differences in complexity. Complexity was increased in cases compared with controls during wake, but this reversed during NREM sleep. In both wake and sleep, microstate topography arises from cortical neurons, while the thalamus may help mediate transitions between states. The wake EEG is dominated by alpha activity, which is organized in part by the pulvinar nucleus of the thalamus (26). NREM EEG is dominated by slow oscillations and sleep spindles that rely on a different set of thalamic nuclei including the thalamic reticular nucleus (37,38). State-dependent differences in complexity suggest distinct and dissociable functional abnormalities in the pulvinar and thalamic reticular nuclei in patients with schizophrenia. This is consistent with postmortem studies of schizophrenia that have shown abnormalities in these nuclei (39,40)

Limitations

The current study has multiple limitations. The cross-sectional design means that this study could not assess relationships between microstates and disease progression or remission. The patients in this study were long-term inpatients and therefore are not fully representative of the range of phenotypes in schizophrenia. EEG provides low-resolution information about the spatial distribution of electrical activity in the brain, and the biological underpinnings of EEG microstate parameters are incompletely understood. Despite these shortcomings, the data presented here provide evidence for sleep-related microstate abnormalities in patients with schizophrenia.

ACKNOWLEDGMENTS AND DISCLOSURES

This work was supported by the Stanley Center at the Broad Institute of Harvard and Massachusetts Institute of Technology, National Institute of Mental Health (Grant Nos. R01 MH115045 and R01 MH118298 [to JQP], R03 MH108908 [to SP], and K23MH118565 to [MM]), National Institute of Neurological Disorders and Stroke (Grant No. NS108874 [to JQP]), National Heart, Lung, and Blood Institute (Grant No. R01 HL146339 [to SP]), National Institute on Minority Health and Health Disparities (Grant Nos. R21 MD012738 and. R21 HL145492 [to SP]), and Top Talent Support Program for Young and Middle-Aged People of Wuxi Health Committee (Grant No. HB2020077 [to JW]). The funders had no role in study design, data collection and interpretation, or the decision to submit the work for publication.

MM and SMP wrote the main manuscript text and prepared the figures. CJ and the GRINS Consortium performed the research. SMP, LAW, NK, YW, and MM analyzed the data. JW, JQP, CJ, and the GRINS Consortium edited the manuscript. All authors reviewed the manuscript.

We thank Stephanie A. Marvin for manual scoring of all GRINS sleep studies.

The authors report no biomedical financial interests or potential conflicts of interest.

ARTICLE INFORMATION

From the Department of Psychiatry, McLean Hospital, Harvard Medical School, Belmont, Massachusetts (MM); Affiliated Wuxi Mental Health Center of Jiangnan University, Wuxi, Jiangsu, China (CJ, JW); Stanley Center for Psychiatric Research, Broad Institute of MIT and Harvard, Cambridge, Massachusetts (LAW, YW, JQP, SMP); and the Department of Psychiatry, Brigham and Women's Hospital, Harvard Medical School, Boston, Massachusetts (NK, SMP).

GRINS Consortium members: Clinical Research Team—Jun Wang, Chenguang Jiang, Guanchen Gai, Kai Zou, Zhe Wang, Xiaoman Yu, Guoqiang Wang, Shuping Tan, Michael Murphy, Mei Hua Hall, Wei Zhu, and

Zhenhe Zhou; Molecular Genetics—Lu Shen, Shenying Qin, and Hailiang Huang; Electrophysiology data analyses—Nataliia Kozhemiako, Lei A Wang, Yining Wang, Lin Zhou, Shen Li, Jun Wang, Robert Law, Minitrios Mylonas, Michael Murphy, Robert Stickgold, Dara Manoach, Mei-Hua Hall, Jen Q. Pan, and Shaun M. Purcell; Project management—Zhenglin Guo, Sinead Chapman, Hailiang Huang, Jun Wang, Chenaugnag Jiang, Zhenhe Zhou, and Jen Q. Pan; Principal Investigators—Mei-Hua Hall, Hailiang Huang, Dara Manoach, Jen Q. Pan, Shaun M. Purcell, and Zhenhe Zhou.

MM and CJ contributed equally to this work.

Address correspondence to Michael Murphy, M.D., Ph.D., at mmurphy@mgh.harvard.edu, Jen Q Pan, Ph.D., at jpan@broadinstitute.org, Shaun M Purcell, Ph.D., at smpurcell@bwh.harvard.edu, or Jun Wang, Ph.D., at woodfish828@gmail.com.

Received Apr 23, 2024; revised Jul 25, 2024; accepted Jul 26, 2024.

Supplementary material cited in this article is available online at https://doi.org/10.1016/j.bpsgos.2024.100371.

REFERENCES

1. Friston K, Brown HR, Siemerkus J, Stephan KE (2016): The dysconnection hypothesis (2016). Schizophr Res 176:83–94.
2. Ferrarelli F, Huber R, Peterson MJ, Massimini M, Murphy M, Riedner BA, *et al.* (2007): Reduced sleep spindle activity in schizophrenia patients. Am J Psychiatry 164:483–492.
3. Kozhemiako N, Wang J, Jiang C, Wang LA, Gai G, Zou K, *et al.* (2022): Non-rapid eye movement sleep and wake neurophysiology in schizophrenia. eLife 11:1–33.
4. Manoach DS, Stickgold R (2019): Abnormal sleep spindles, memory consolidation, and schizophrenia. Annu Rev Clin Psychol 15:451–479.
5. Goldstein MR, Peterson MJ, Sanguinetti JL, Tononi G, Ferrarelli F (2015): Topographic deficits in alpha-range resting EEG activity and steady state visual evoked responses in schizophrenia. Schizophr Res 168:145–152.
6. Ramsay IS, Lynn P, Schermitzler B, Sponheim S (2021): Individual alpha peak frequency is slower in schizophrenia and related to deficits in visual perception and cognition. Sci Rep 11:1–9.
7. Murphy M, Öngür D (2019): Decreased peak alpha frequency and impaired visual evoked potentials in first episode psychosis. NeuroImage Clin 22:101693.
8. Lehmann D (1990): Brain electric microstates and cognition: The atoms of thought. In: John ER, editor. Machinery of the Mind. Boston: Birkhäuser, 209–224.
9. Michel CM, Koenig T (2018): EEG microstates as a tool for studying the temporal dynamics of whole-brain neuronal networks: A review. Neuroimage 180:577–593.
10. Tarailis P, Koenig T, Michel CM, Griškova-Bulanova IG (2024): The functional aspects of resting EEG microstates: A systematic review. Brain Topogr 37:181–217.
11. Custo A, Van De Ville D, Wells WM, Tomescu MI, Brunet D, Michel CM (2017): Electroencephalographic resting-state networks: Source localization of microstates. Brain Connect 7:671–682.
12. Rieger K, Diaz Hernandez LD, Baenninger A, Koenig T (2016): 15 years of microstate research in schizophrenia – Where are we? A meta-analysis. Front Psychiatry 7:1–7.
13. da Cruz JR, Favrod O, Roinishvili M, Chkonia E, Brand A, Mohr C, *et al.* (2020): EEG microstates are a candidate endophenotype for schizophrenia. Nat Commun 11:1–11.
14. Murphy M, Stickgold R, Öngür D (2020): Electroencephalogram microstate abnormalities in early-course psychosis. Biol Psychiatry Cogn Neurosci Neuroimaging 5:35–44.
15. Brodbeck V, Kuhn A, von Wegner F, Morzelewski A, Tagliazucchi E, Borisov S, *et al.* (2012): EEG microstates of wakefulness and NREM sleep. Neuroimage 62:2129–2139.
16. Bréchet L, Brunet D, Perogamvros L, Tononi G, Michel CM (2020): EEG microstates of dreams. Sci Rep 10:1–9.
17. Kay SR, Fiszbein A, Opler LA (1987): The Positive and Negative Syndrome Scale (PANSS) for schizophrenia. Schizophr Bull 13:261–276.
18. Purcell SM, Manoach DS, Demanuele C, Cade BE, Mariani S, Cox R, *et al.* (2017): Characterizing sleep spindles in 11,630 individuals from the National Sleep Research Resource. Nat Commun 8:1–16.
19. Murphy M, Wang J, Jiang C, Wang LA, Kozhemiako N, Wang Y, *et al.* (2024): A potential source of bias in group-level EEG microstate analysis. Brain Topogr 37:232–242.
20. Bréchet L, Brunet D, Birot G, Gruetter R, Michel CM, Jorge J (2019): Capturing the spatiotemporal dynamics of self-generated, task-initiated thoughts with EEG and fMRI. Neuroimage 194:82–92.
21. Welch TA (1984): A technique for high-performance data compression. Computer (Long Beach Calif) 17(17):8–19.
22. Freedman D, Lane D, Freedman D (1983): A nonstochastic interpretation of reported significance levels. J Bus Econ Stat 1:292–298.
23. Winkler AM, Ridgway GR, Webster MA, Smith SM, Nichols TE (2014): Permutation inference for the general linear model. Neuroimage 92:381–397.
24. Nunez PL, Srinivasan R (2006): Electric Fields of the Brain. Oxford: Oxford University Press.
25. Milz P, Pascual-Marqui RD, Achermann P, Kochi K, Faber PL (2017): The EEG microstate topography is predominantly determined by intracortical sources in the alpha band. Neuroimage 162:353–361.
26. Hughes SW, Crunelli V (2005): Thalamic mechanisms of EEG alpha rhythms and their pathological implications. Neuroscientist 11:357–372.
27. Halgren M, Ulbert I, Bastuji H, Fabó D, Erőss L, Rey M, *et al.* (2019): The generation and propagation of the human alpha rhythm. Proc Natl Acad Sci U S A 116:23772–23782.
28. Bazhenov M, Timofeev I, Steriade M, Sejnowski T (2000): Spiking-bursting activity in the thalamic reticular nucleus initiates sequences of spindle oscillations in thalamic networks. J Neurophysiol 84:1076–1087.
29. Timofeev I, Steriade M (1996): Low-frequency rhythms in the thalamus of intact-cortex and decorticated cats. J Neurophysiol 76:4152–4168.
30. Tononi G, Cirelli C (2006): Sleep function and synaptic homeostasis. Sleep Med Rev 10:49–62.
31. Britz J, Van De Ville D, Michel CM (2010): BOLD correlates of EEG topography reveal rapid resting-state network dynamics. Neuroimage 52:1162–1170.
32. Siclari F, Baird B, Perogamvros L, Bernardi G, LaRocque JJ, Riedner B, *et al.* (2017): The neural correlates of dreaming. Nat Neurosci 20:872–878.
33. Murphy M, Riedner BA, Huber R, Massimini M, Ferrarelli F, Tononi G (2009): Source modeling sleep slow waves. Proc Natl Acad Sci U S A 106:1608–1613.
34. Schabus M, Dang-Vu TT, Albouy G, Balteau E, Boly M, Carrier J, *et al.* (2007): Hemodynamic cerebral correlates of sleep spindles during human non-rapid eye movement sleep. Proc Natl Acad Sci U S A 104:13164–13169.
35. Irisawa S, Isotani T, Yagyu T, Morita S, Nishida K, Yamada K, *et al.* (2006): Increased omega complexity and decreased microstate duration in nonmedicated schizophrenic patients. Neuropsychobiology 54:134–139.
36. Fernández A, Gómez C, Hornero R, López-Ibor JJ (2013): Complexity and schizophrenia. Prog Neuropsychopharmacol Biol Psychiatry 45:267–276.
37. Halassa MM, Siegle JH, Ritt JT, Ting JT, Feng G, Moore CI (2011): Selective optical drive of thalamic reticular nucleus generates thalamic bursts and cortical spindles. Nat Neurosci 14:1118–1120.
38. David F, Schmiedt JT, Taylor HL, Orban G, Di Giovanni G, Uebele VN, *et al.* (2013): Essential thalamic contribution to slow waves of natural sleep. J Neurosci 33:19599–19610.
39. Court J, Spurden D, Lloyd S, McKeith I, Ballard C, Cairns N, *et al.* (1999): Neuronal nicotinic receptors in dementia with Lewy bodies and schizophrenia: α-Bungarotoxin and nicotine binding in the thalamus. J Neurochem 73:1590–1597.
40. Byne W, Fernandes J, Haroutunian V, Huacon D, Kidkardnee S, Kim J, *et al.* (2007): Reduction of right medial pulvinar volume and neuron number in schizophrenia. Schizophr Res 90:71–75.
41. Wallwork RS, Fortgang R, Hashimoto R, Weinberger DR, Dickinson D (2012): Searching for a consensus five-factor model of the Positive and Negative Syndrome Scale for schizophrenia. Schizophr Res 137:246–250.